

2017 Winter School

Discussions on X-ray Tomography Using Sandwich Detectors

2017. 1. 10

Ho Kyung Kim

hokyung@pusan.ac.kr

Pusan National University

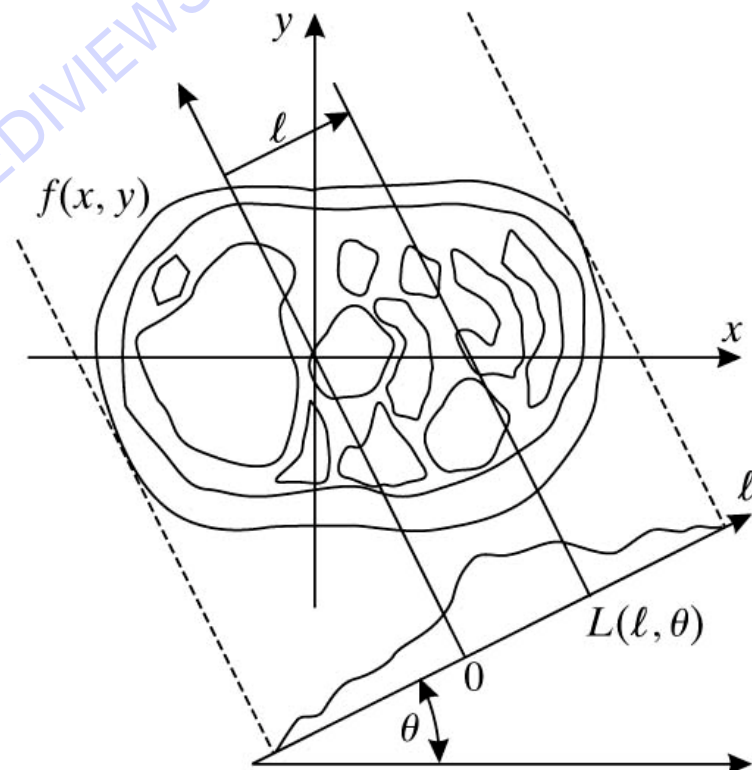
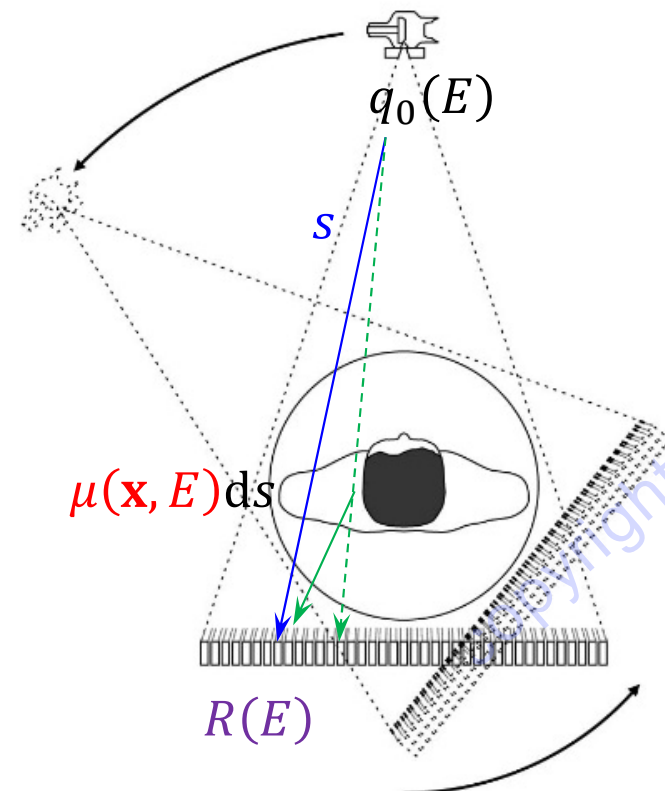
Outline

- Conspicuity
- Microtomography with a sandwich detector
- Issues in the use of sandwich detectors

Forward model

$$d(\xi; s) = Xka^2(1 + \text{SPR}) \int_0^\infty q_0(E) e^{-\int_s \mu(x, E) ds} R(E) dE$$

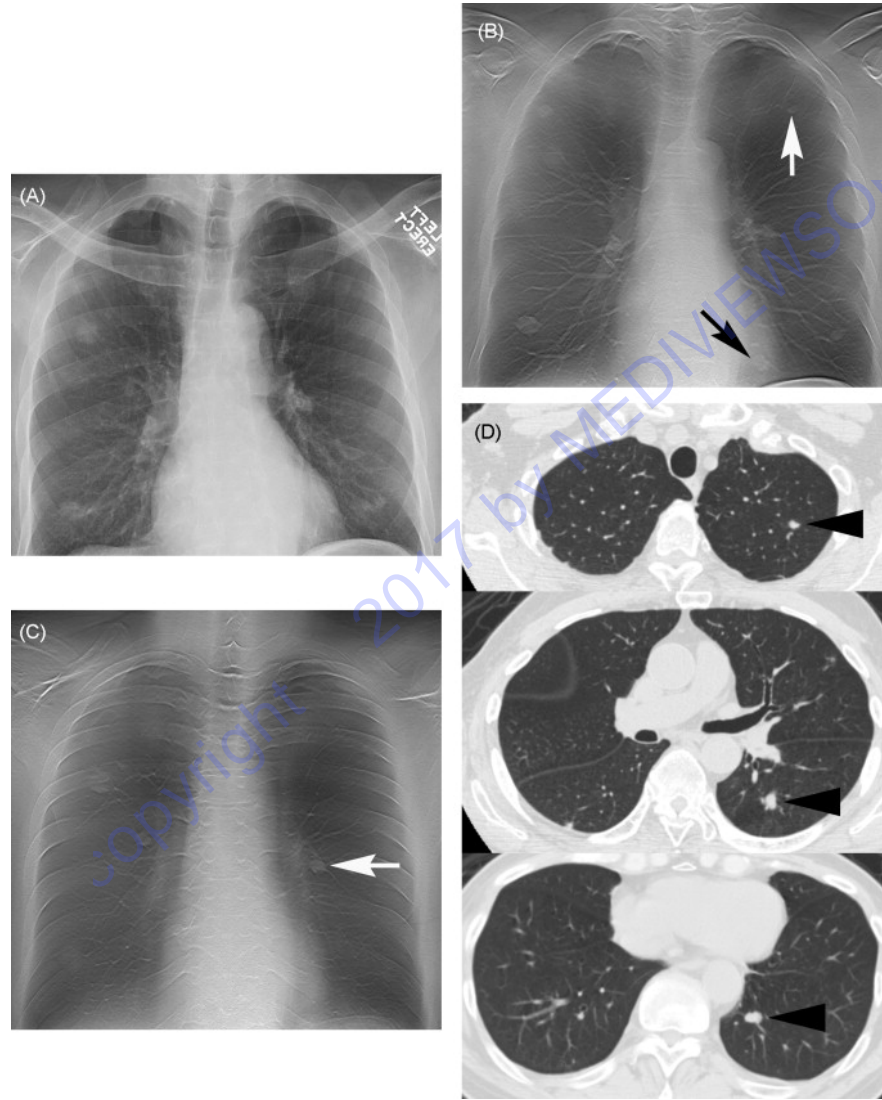
Anatomical background noise
Quantum noise
Conspicuity



(Images taken from) J. L. Prince & J. M. Links |
Medical Imaging Signals and Systems | Pearson Education, Inc. | 2006

Depth discrimination

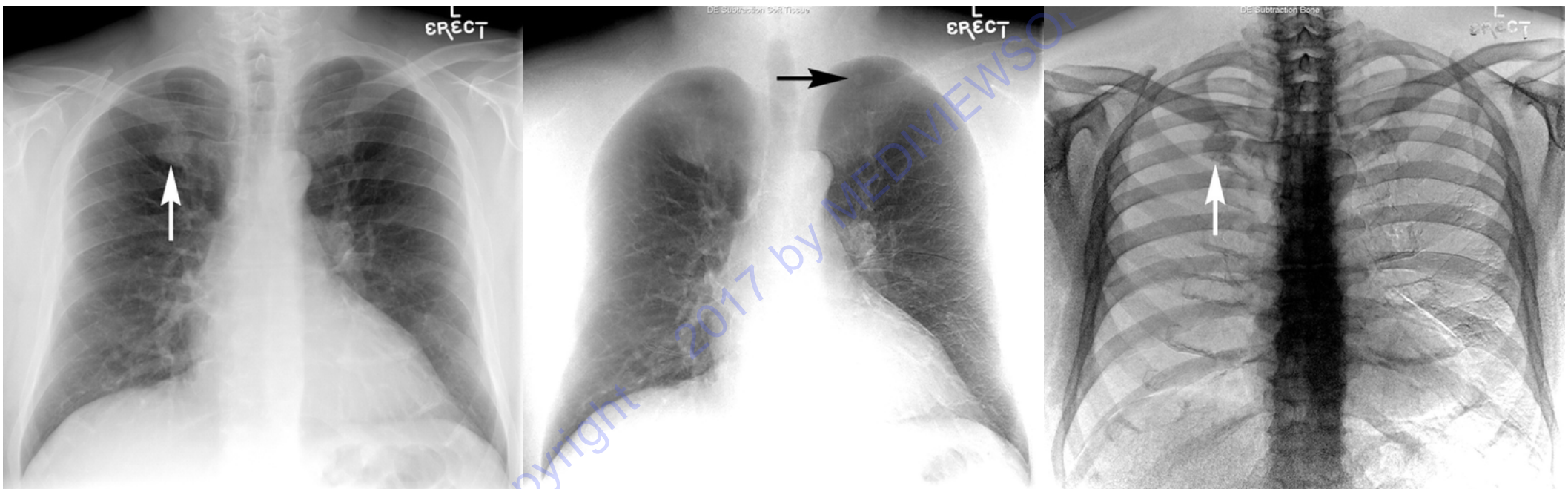
Digital tomosynthesis (DTS)
Computed tomography (CT)



(Images taken from) J. T. Dobbins III & H. P. McAdams | Eur. J. Radiol. | 2009

Energy discrimination

Digital radiography (DR)
Dual-energy imaging (DEI)



(Images taken from) H. P. McAdams *et al.* | Radiology | 2006

DE reconstruction

- Basis material decomposition

$$\mu(E) \approx \mu_{\text{pe}}(E) + \mu_{\text{cs}}(E) \approx K_{\text{pe}} \frac{\rho}{A} Z^4 E^{-3} + K_{\text{cs}} \frac{\rho}{A} Z f_{\text{KN}}(E) = a_{\text{pe}} E^{-3} + a_{\text{cs}} f_{\text{KN}}(E)$$

$$\mu(E) = a_1 \mu_1(E) + a_2 \mu_2(E)$$

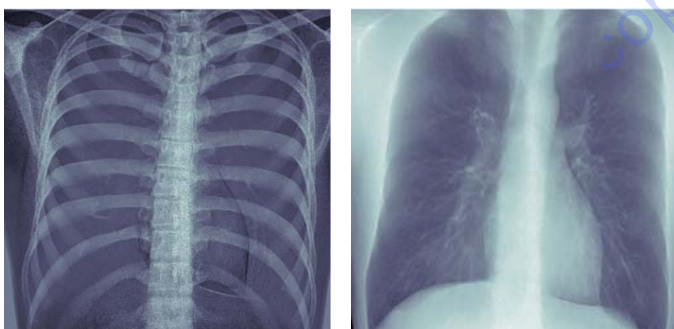
R. E. Alvarez & A. Macovski | PMB | 1976

- Weighted log-subtraction

$$p = \ln \frac{I_0}{I} = \sum_j \mu_j t_j$$

$$t_j = |w_j p^L - p^H|$$

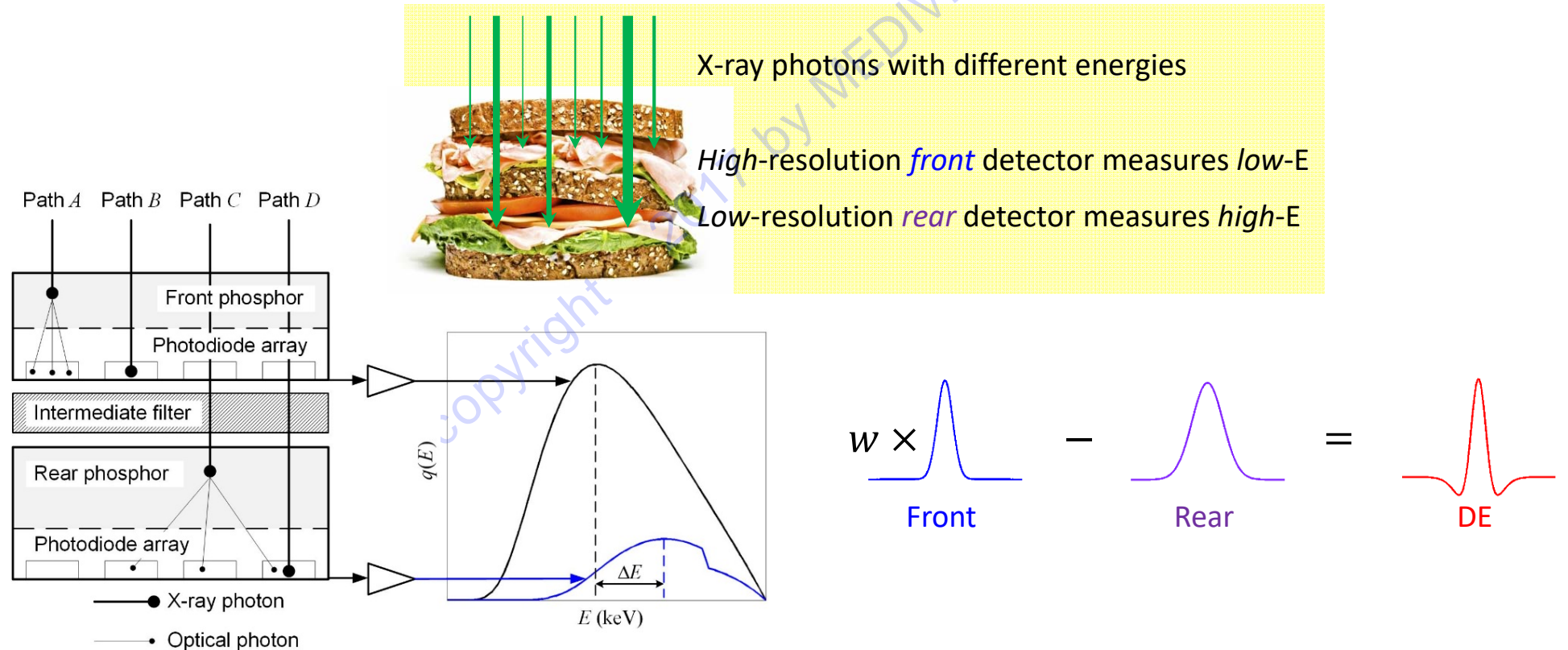
for two materials (e.g., j = bone or soft tissue)



From a commercial system (GE Definix 8000)

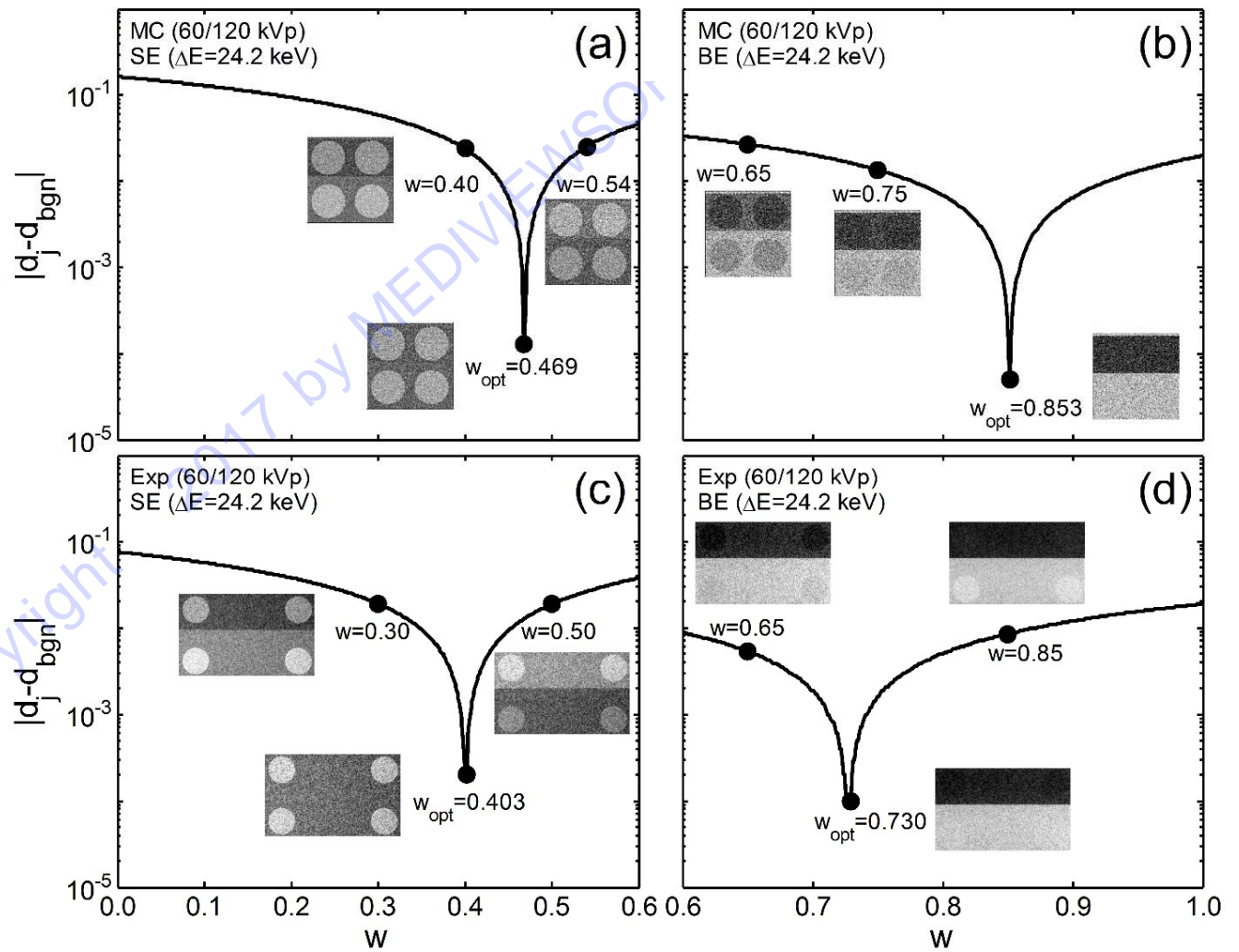
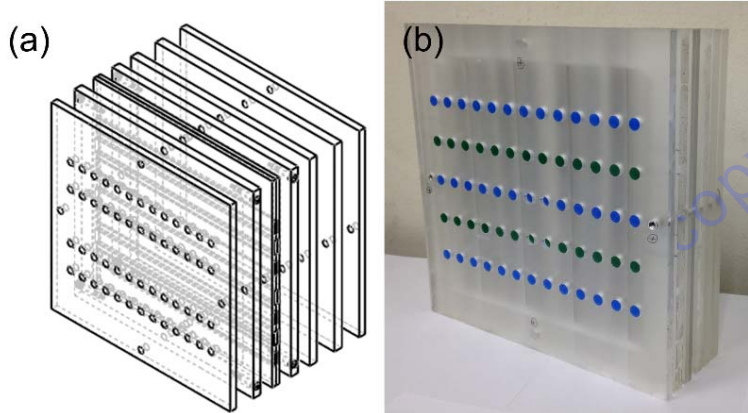
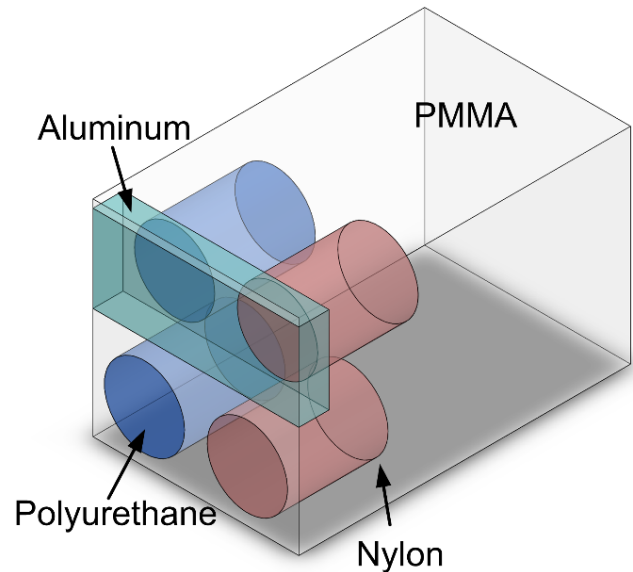
Concept of the sandwich detector

- The *beam hardening* through the front detector layer makes different energy measurements, thereby DE imaging
- Different thicknesses* of detector layers make *edge-enhancement* in the resulting DE images

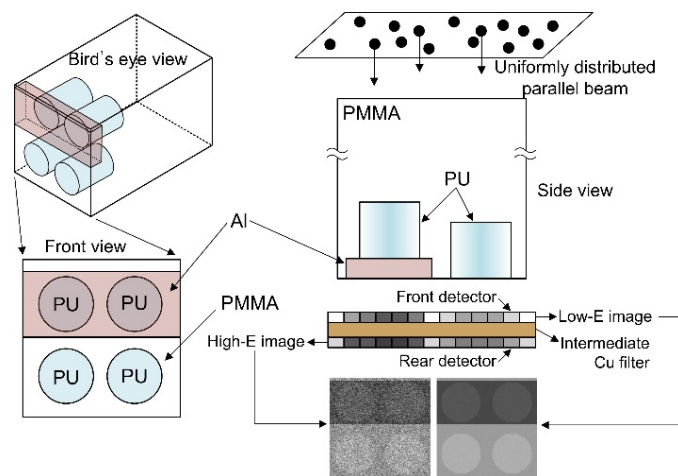


Motion artifact
Contrast & noise
Energy separation
Intermediate filter
Edge enhancement

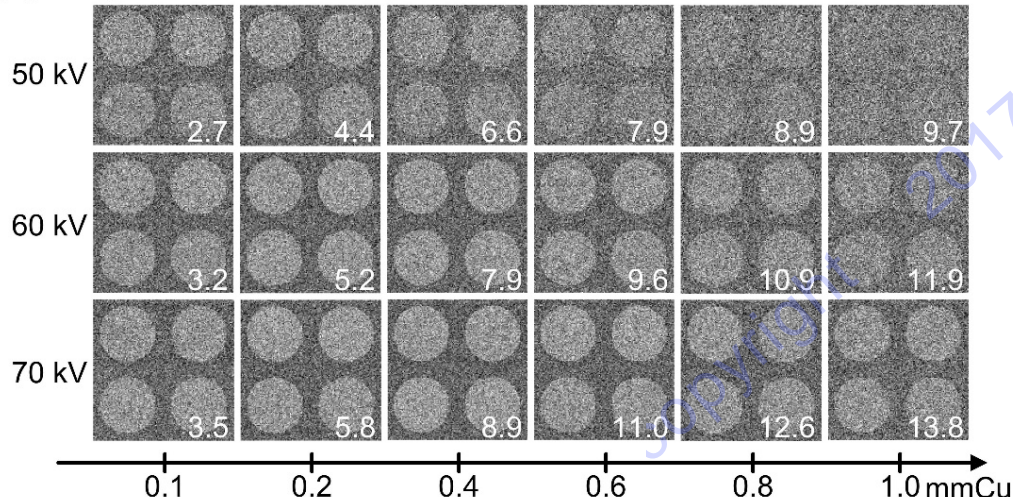
Determination of tissue cancellation parameters



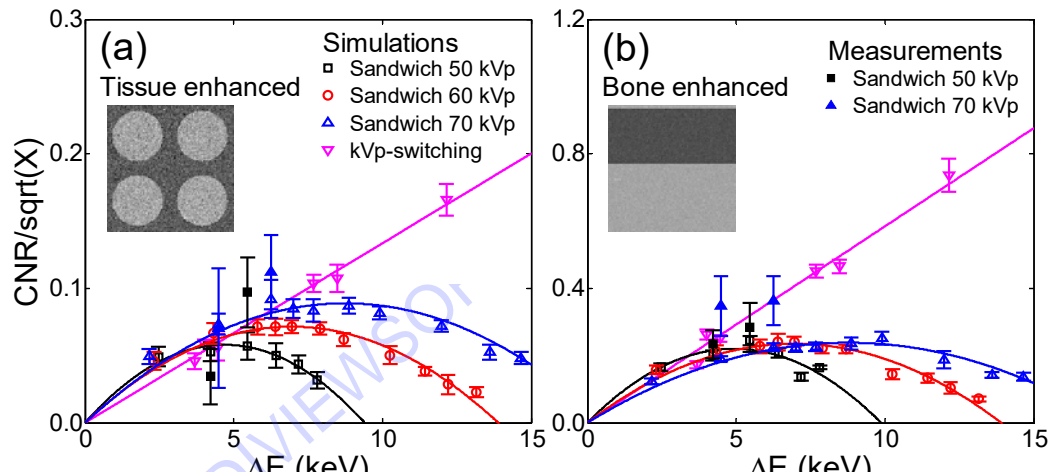
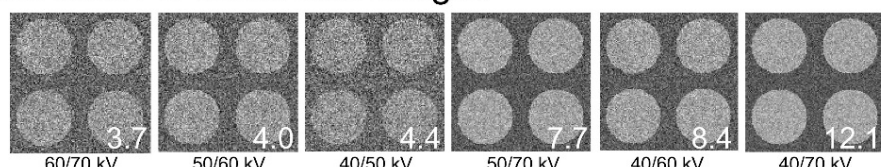
Phantom study



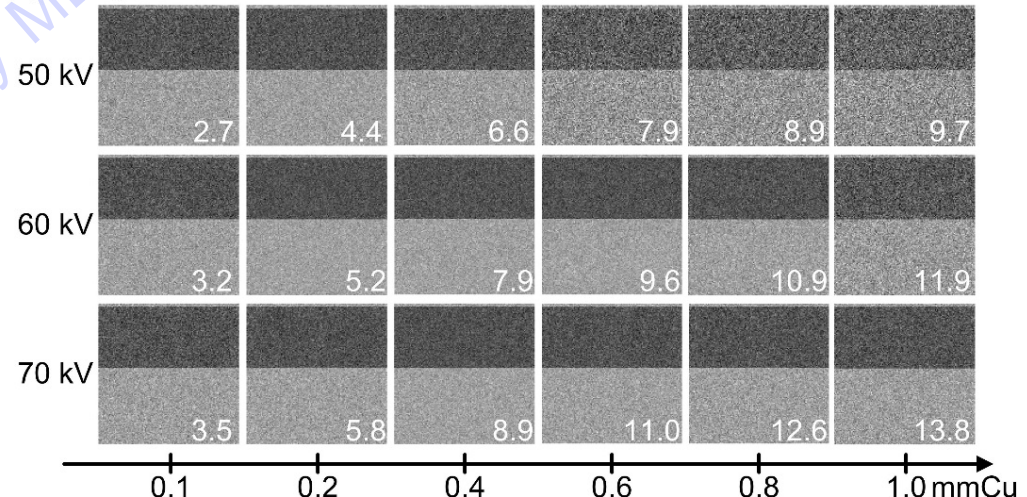
(a) Single-shot PU-enhanced images



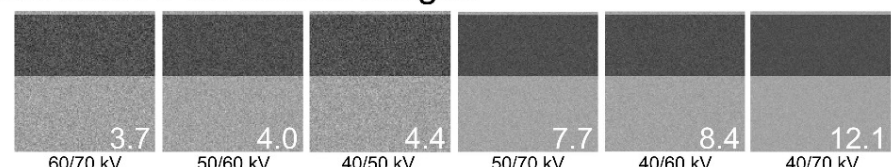
(b) Dual-shot PU-enhanced images



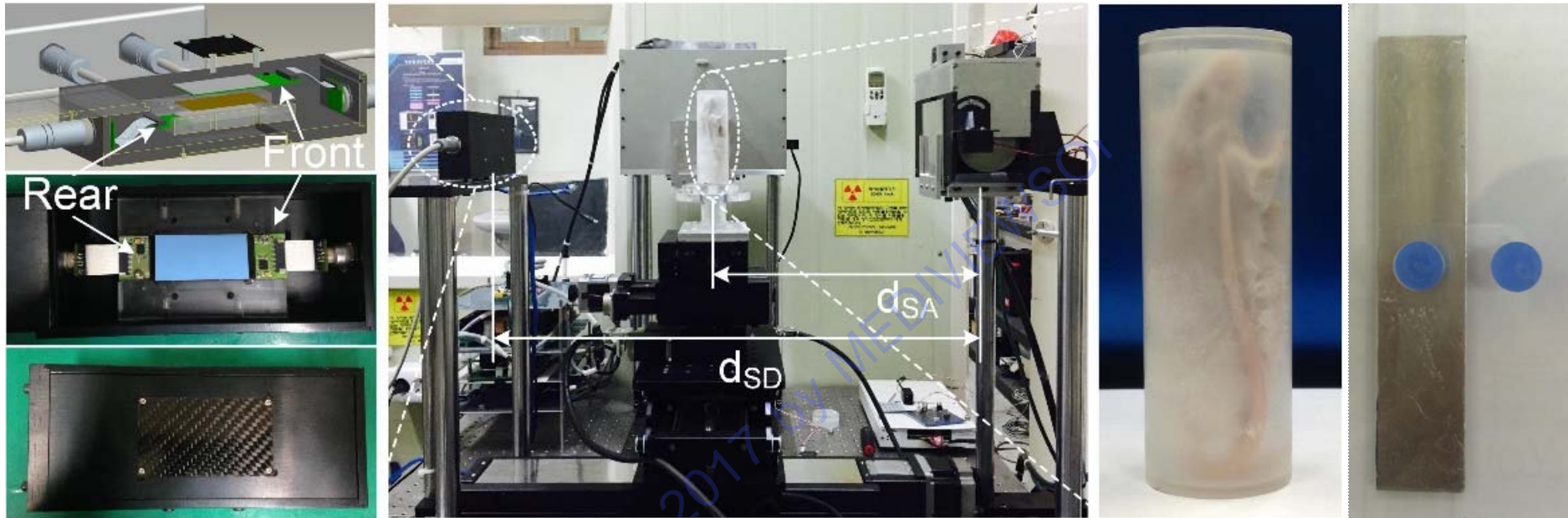
(a) Single-shot AI-enhanced images



(b) Dual-shot AI-enhanced images

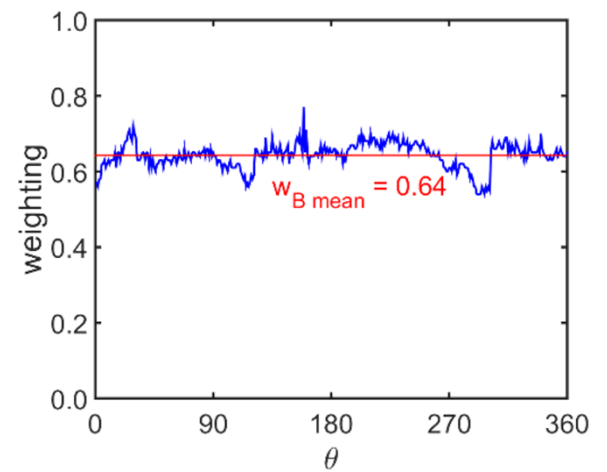
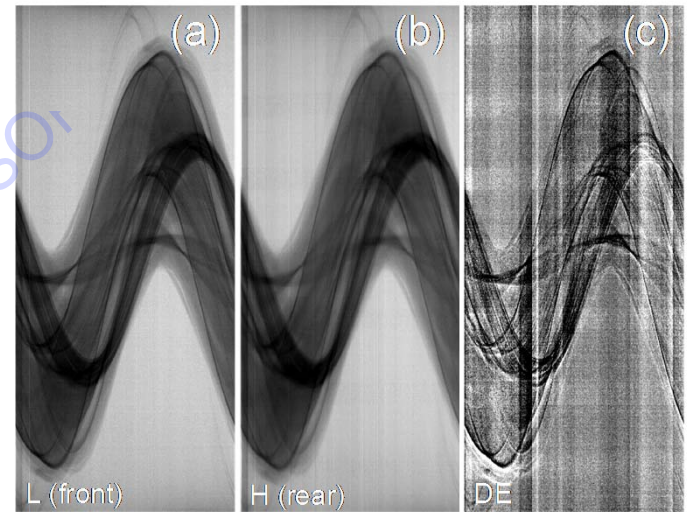
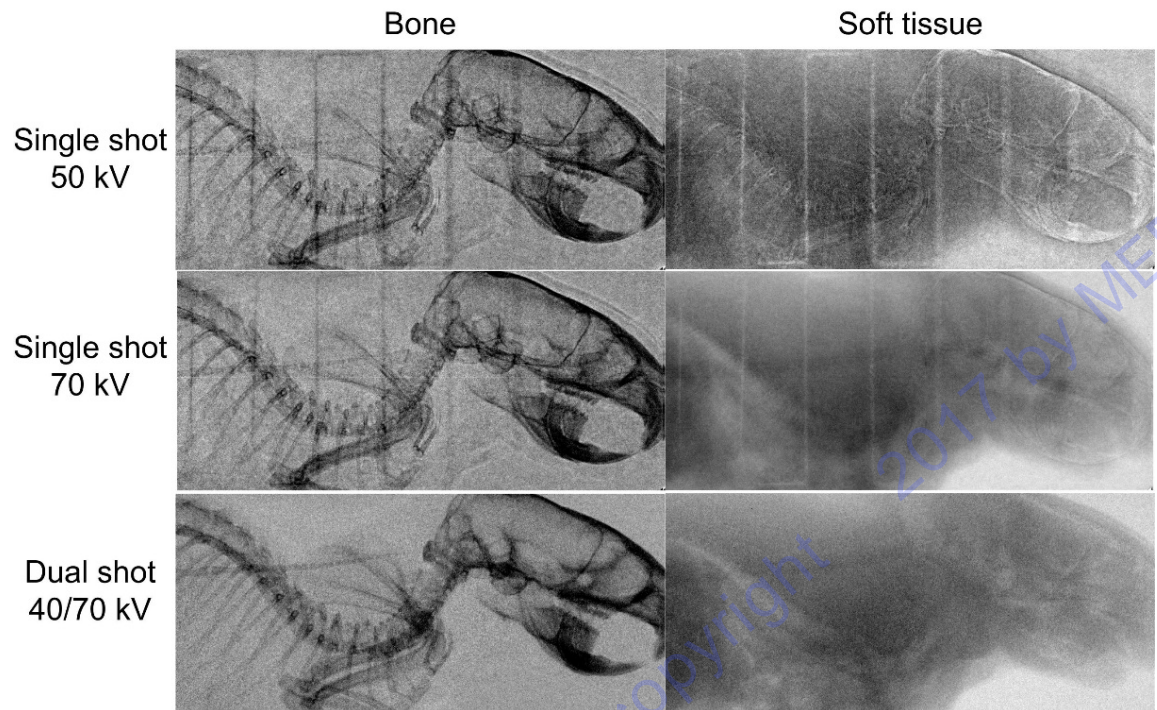


Bench-top system

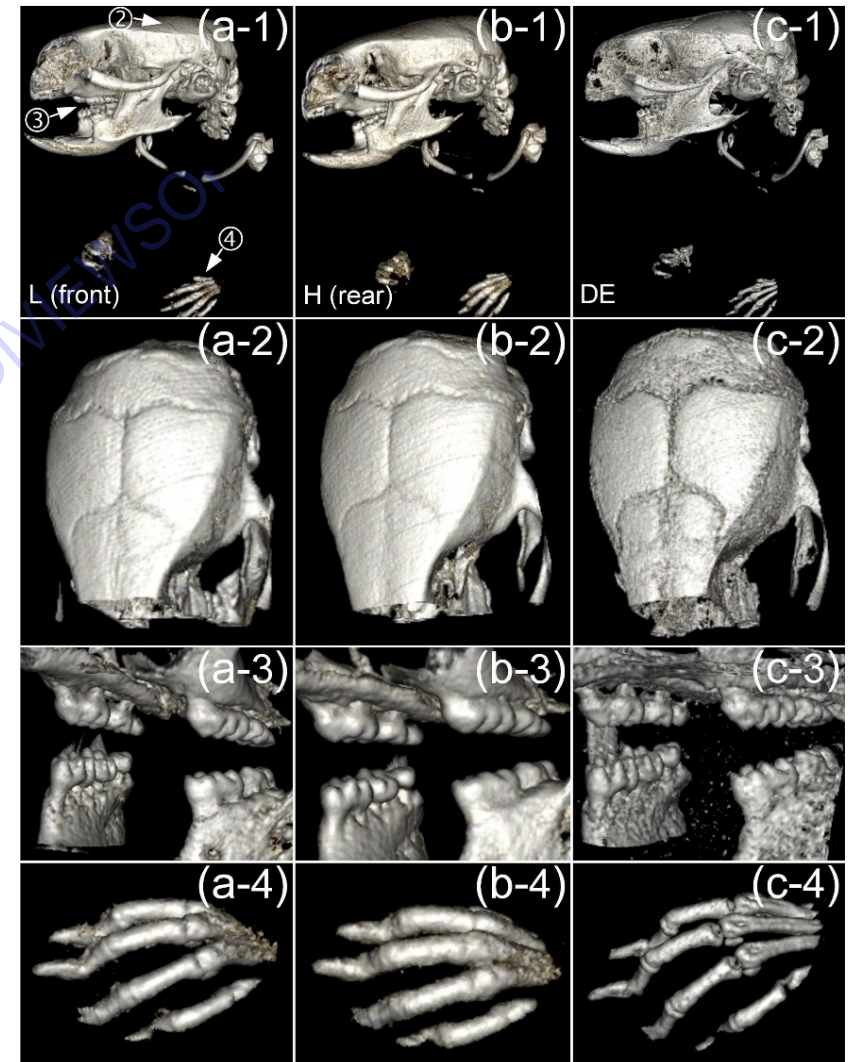
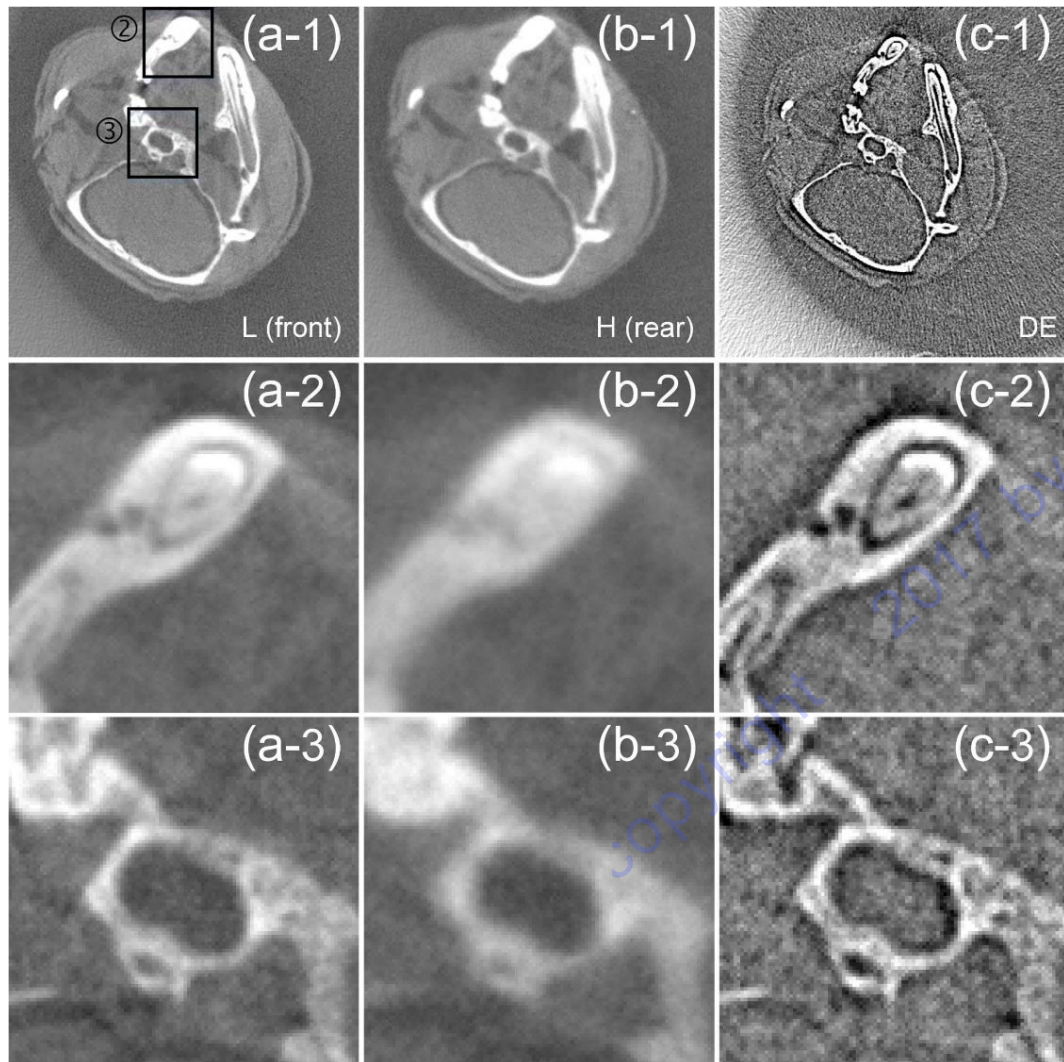


Detector	$\text{Gd}_2\text{O}_2\text{S:Tb}$ ($\sim 34 \text{ mg cm}^{-2}$) / CMOS PD / Cu / $\text{Gd}_2\text{O}_2\text{S:Tb}$ ($\sim 67 \text{ mg cm}^{-2}$) / CMOS PD
X-ray source	W anode / 50 Watts
Acquisition	Continuous irradiation
Reconstruction	FDK with the Hanning apodization filter

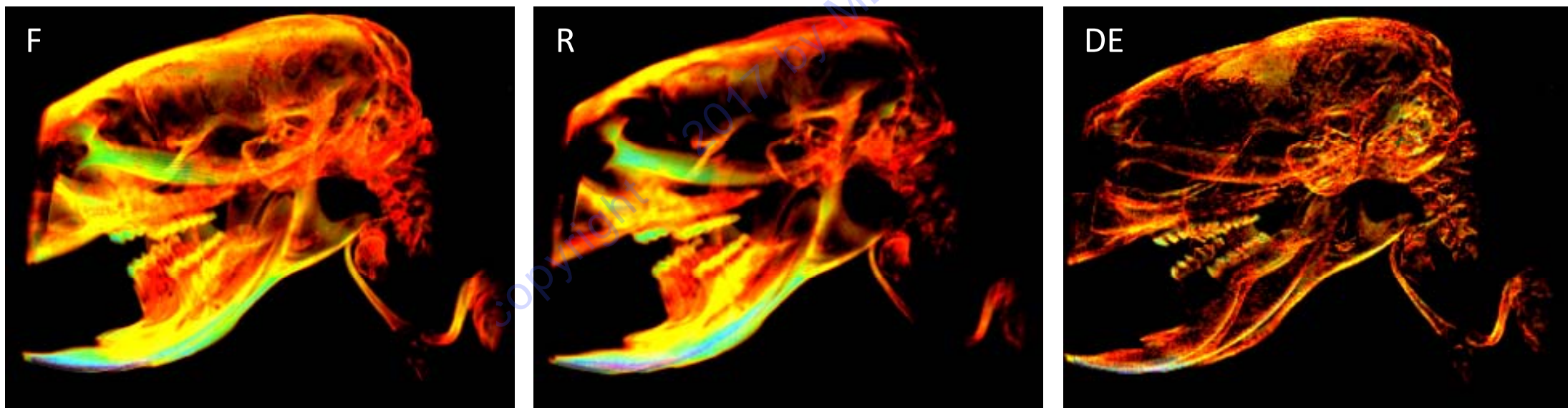
Projections



Tomography



- Total dose to mouse = 0.128 Gy
 - Typ. CT dose to mice from 0.014 Gy to 0.226 Gy [S. Carlson *et al.* | Mol. Imaging Biol. | 2007]
 - Mouse can recover if a daily exposure is less than 0.5 Gy [R. H. Mole | Br. J. Radiol. | 1957]



Linear approximation of imaging theory

Log transformation

$$p(x) = \mathcal{L}\{q(x) * g(x)\}$$

$$\bar{p}(x) = \bar{\lambda} \bar{q} \bar{g} L(x) \text{ with a constraint of } \int_{-\infty}^{\infty} L(x) dx = 1$$

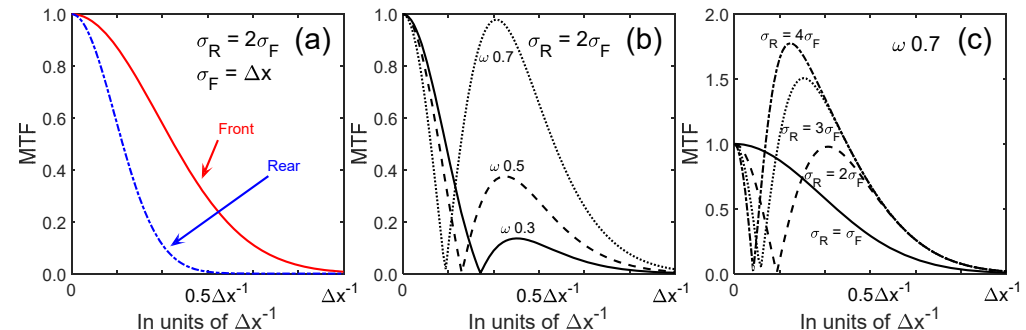
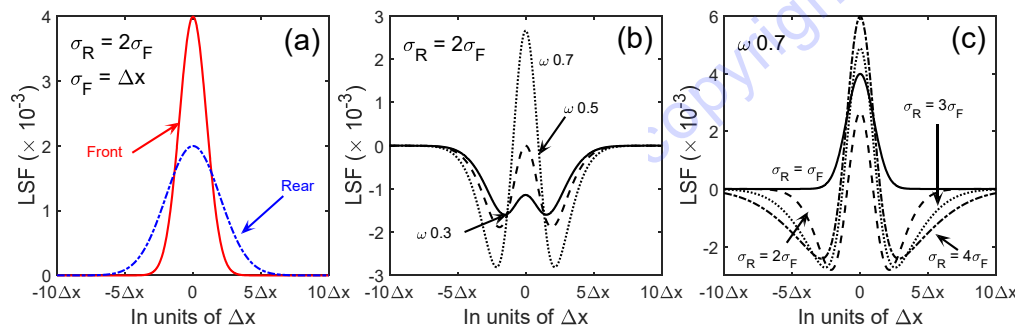
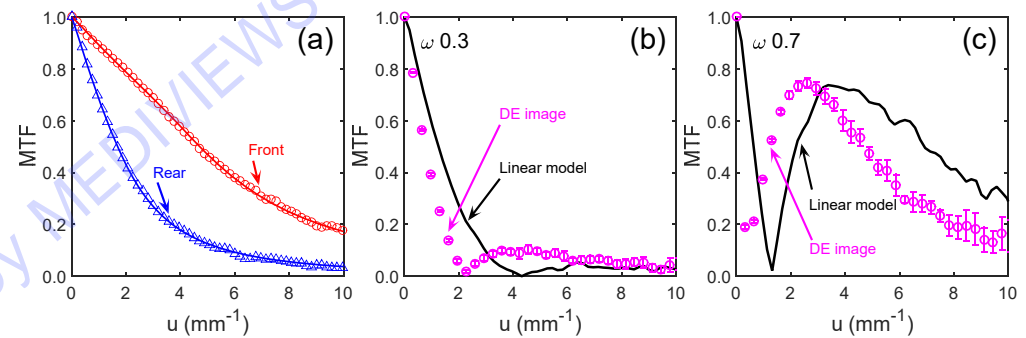
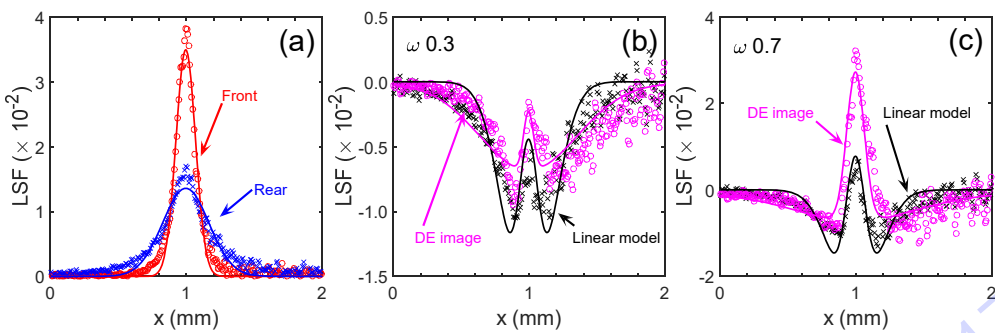
where $\bar{\lambda} \approx \frac{1}{\bar{d}}$ & $\bar{g} = \left| \frac{\partial \bar{d}}{\partial \bar{q}} \right|$

DE imaging

$$p^{DE}(x) = |w p^L(x) - p^H(x)|$$

$$\text{MTF}^{DE}(u) = \left| \mathcal{F} \left\{ \frac{w L^L(x) - L^H(x)}{\int_{-\infty}^{\infty} [w L^L(x) - L^H(x)] dx} \right\} \right| = \left| \frac{w \text{MTF}^L(u) - \text{MTF}^H(u)}{w - 1} \right|$$

- Lost of contrast in large-area content
- Boost-up of contrast in mid/high-spatial freq. content



Extension to FBP & Halo effect

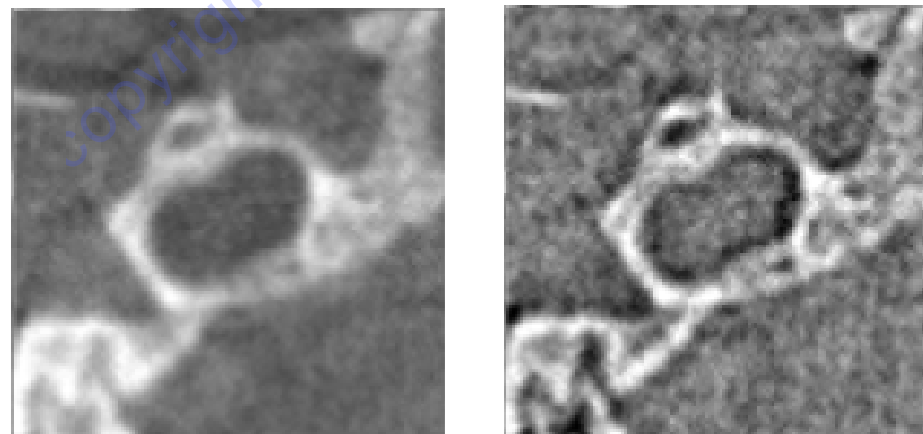
Filtered projection

$$\hat{p}(\xi) = \bar{\lambda} \bar{q} \bar{g} L(\xi) * h(\xi) = \bar{\lambda} \bar{q} \bar{g} \hat{L}(\xi)$$

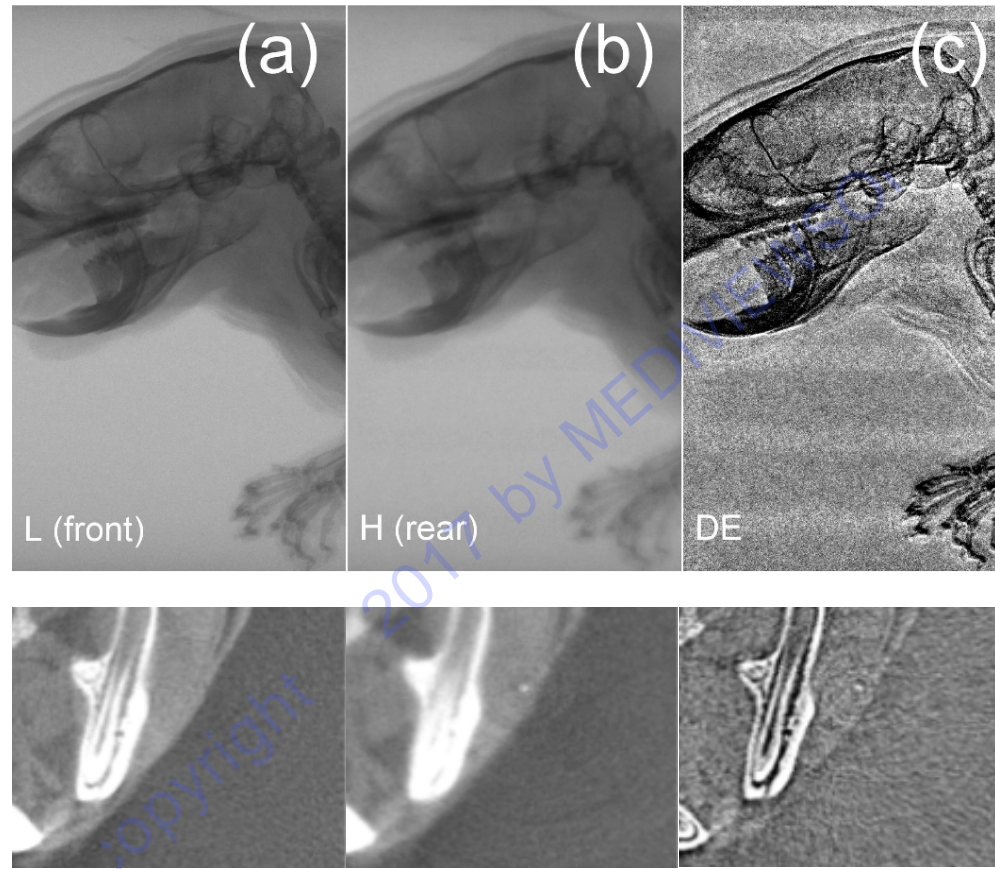
Back-projection $\hat{f}(\mathbf{x}) = a \int_0^{2\pi} \hat{p}(\xi; \theta) \Big|_{\xi=\mathbf{x}\cdot\boldsymbol{\theta}} d\theta = a \bar{\lambda} \bar{q} \bar{g} \int_0^{2\pi} \hat{L}(\mathbf{x} \cdot \boldsymbol{\theta}; \theta) d\theta$

$$\text{MTF}(\mathbf{u}) = \mathcal{F} \left\{ \frac{\hat{f}(\mathbf{x})}{\int_{-\infty}^{\infty} \hat{f}(\mathbf{x}) d\mathbf{x}} \right\} = \mathcal{F} \left\{ \int_0^{2\pi} \hat{L}(\mathbf{x} \cdot \boldsymbol{\theta}; \theta) d\theta \right\}$$

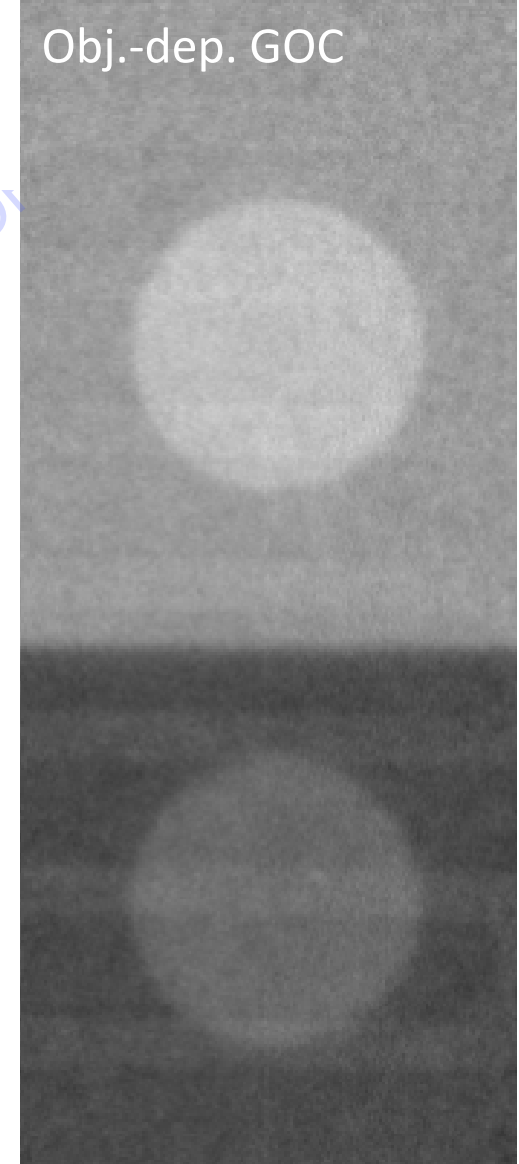
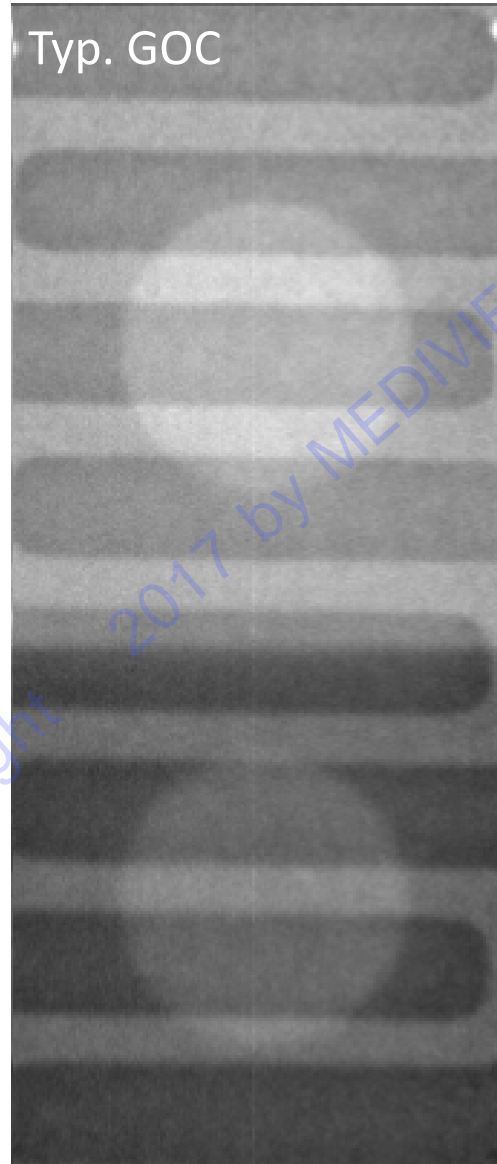
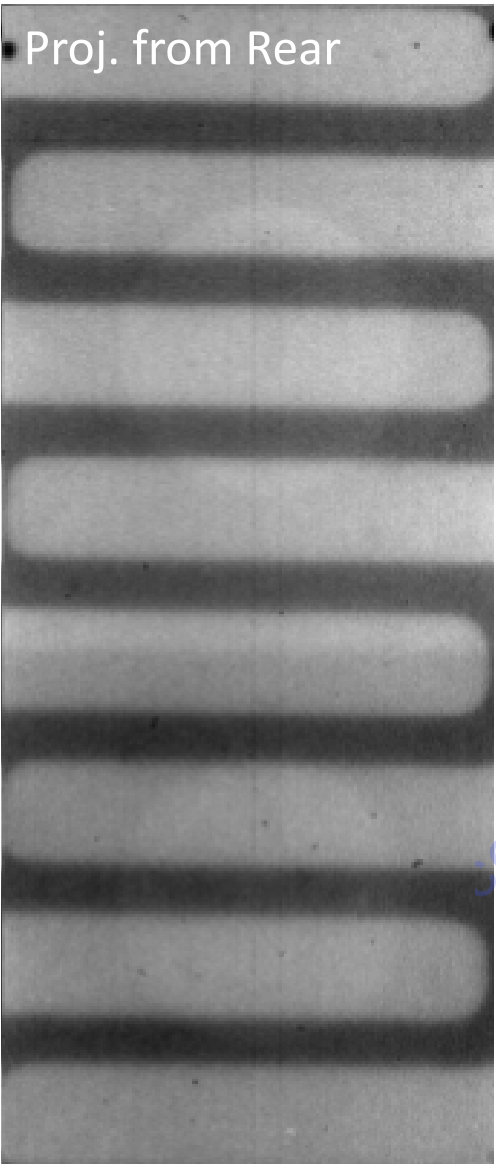
$$\text{MTF}^{DE}(\mathbf{u}) = \left| \frac{\bar{w} \text{MTF}^L(\mathbf{u}) - \text{MTF}^H(\mathbf{u})}{\bar{w} - 1} \right|$$



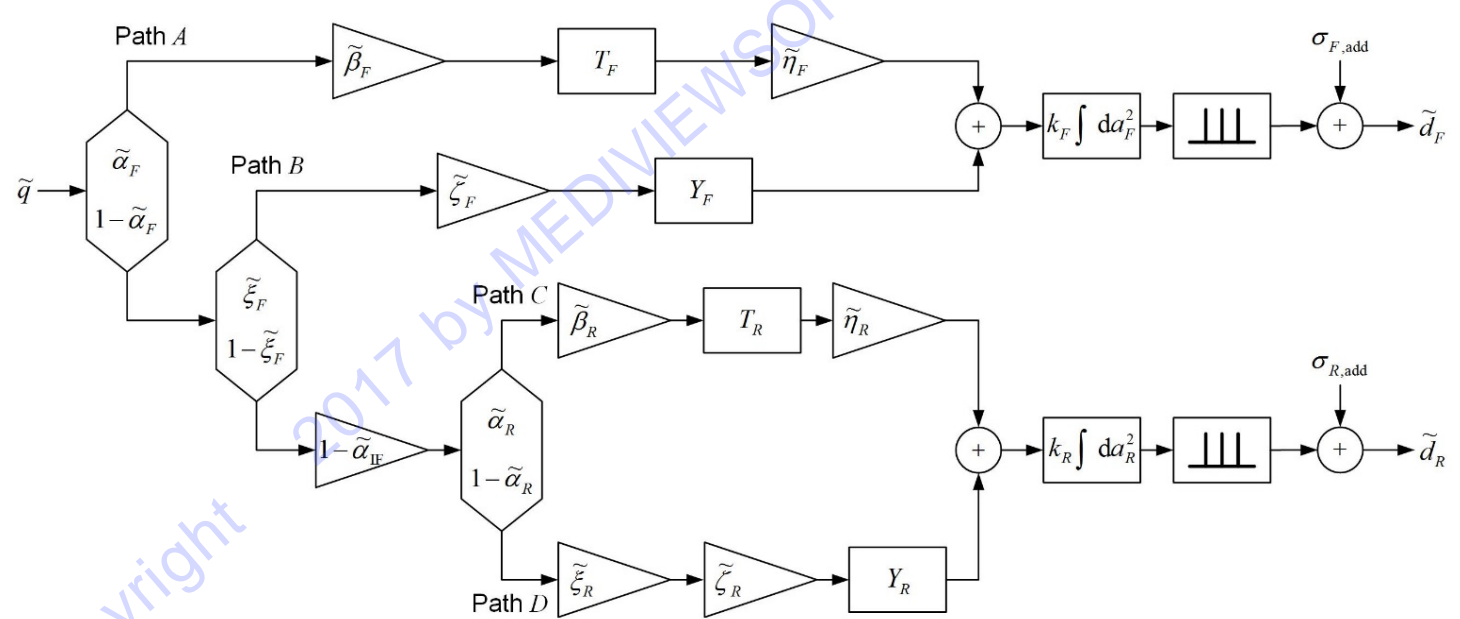
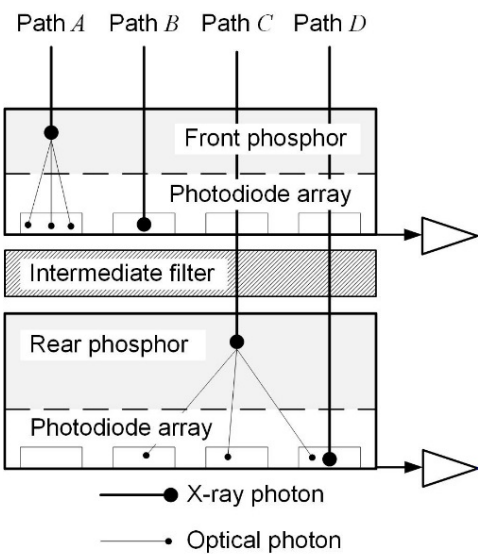
Gain & offset correction & Ring artifacts



$$d(\xi) = c(\xi) \int_0^{\infty} \bar{q}(E, \xi) \alpha(E, \xi) R(E, \xi) \, dE$$



Signal & noise



J. C. Han *et al.* | Cur. Appl. Phys. | 2014

D. W. Kim *et al.* | Proc. SPIE | 2015

D. W. Kim *et al.* | J. Instrum. | 2016

$$\text{MTF}_j(u) = \frac{[\bar{m}_{j,\text{indirect}} T_j(u) + \hat{\alpha}_j \bar{m}_{j,\text{direct}} Y_j(u)] |\text{sinc}(au)|}{\bar{m}_{j,\text{indirect}} + \hat{\alpha}_j \bar{m}_{j,\text{direct}}}$$

$$\bar{d}_j = ka^2 \bar{q} \bar{\tau}_j (\bar{m}_{j,\text{indirect}} + \hat{\alpha}_j \bar{m}_{j,\text{direct}}) = ka^2 \bar{q} \bar{\tau}_j \bar{g}_j$$

$$\bar{\tau}_F = 1 \quad \& \quad \bar{\tau}_R = \hat{\alpha}_F \hat{\xi}_F \hat{\alpha}_{IF}$$

$$\text{DQE}_j(u) = \frac{\bar{d}_j^2 \text{MTF}_j^2(u)}{\bar{q} \text{NPS}_j(u)} = \frac{\text{MTF}_j^2(u)}{\bar{q} [\text{NPS}_j(u)/\bar{d}_j^2]} = \frac{\text{MTF}_j^2(u)}{\bar{q} [W'_{j,\text{indirect}}(u) + W'_{j,\text{direct}} + W'_{j,\text{add}}]}$$

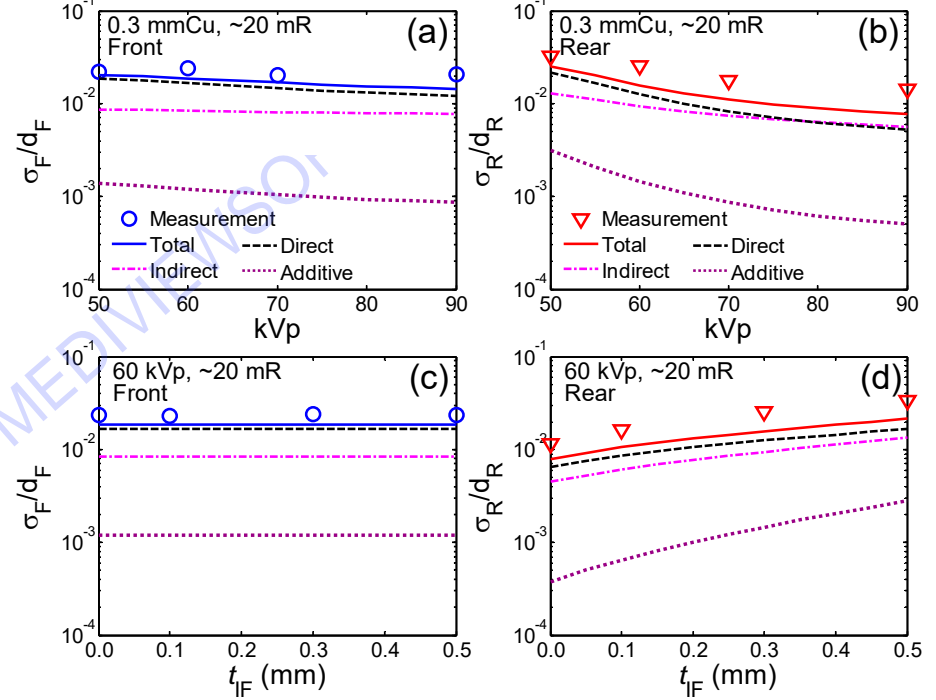
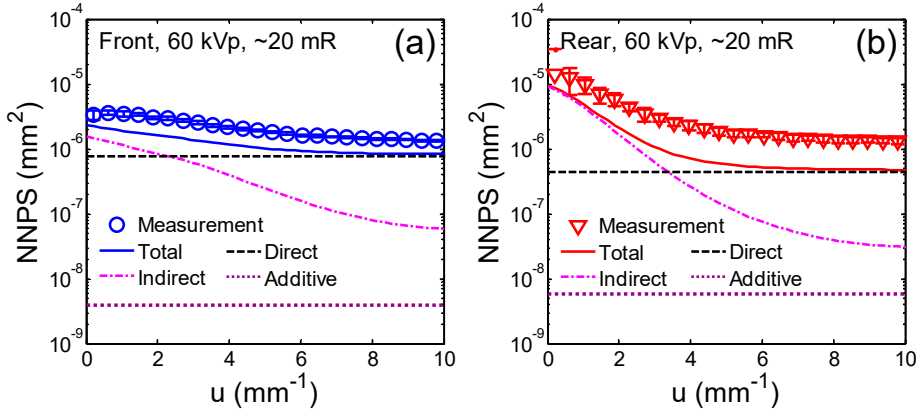
$$W'_{j,\text{indirect}}(u) = \frac{\bar{m}_{j,\text{indirect}}^2}{\bar{q} \bar{\tau}_j \bar{g}_j^2} \left[\frac{1}{\gamma \bar{m}_{j,\text{indirect}}} + \frac{1}{\bar{\alpha}_j} \left(\frac{1}{I_{j,\text{indirect}}} - \frac{1}{\bar{\beta}_j} \right) T_{j,\text{alias}}^2(u) \right]$$

$$W'_{j,\text{direct}}(u) = \frac{\hat{\alpha}_j \bar{m}_{j,\text{direct}}^2}{\gamma \bar{q} \bar{\tau}_j \bar{\xi}_j I_{j,\text{direct}} \bar{g}_j^2}$$

$$W'_{j,\text{add}}(u) = \frac{\bar{\sigma}_{j,\text{add}}^2}{\gamma a^2 \bar{q}^2 \bar{\tau}_j^2 \bar{g}_j^2}$$

$$T_{j,\text{alias}}^2(u) = \sum_{n=0}^{\infty} \sum_{m=0}^{\infty} T_{j,\text{sys}}^2 \left((u, v) \pm \left(\frac{n}{p_x}, \frac{m}{p_y} \right) \right) \Big|_{v=0}$$

Noise



$$\sigma'_{j,indirect} = \frac{\bar{m}_{j,indirect}^2}{\bar{q}\bar{\tau}_j\bar{g}_j^2} \left[\frac{1}{a^2\bar{m}_{j,indirect}} + \frac{1}{a_{j,eff}^2\bar{\alpha}_j} \left(\frac{1}{I_{j,indirect}} - \frac{1}{\bar{\beta}_j} \right) \right]$$

$$\sigma'_{j,direct} = \frac{\hat{\alpha}_j \bar{m}_{j,direct}^2}{a^2 \bar{q} \bar{\tau}_j \bar{\xi}_j I_{j,direct} \bar{g}_j^2}$$

$$\sigma'_{j,add} = \frac{\bar{\sigma}_{j,add}^2}{(a^2 \bar{q} \bar{\tau}_j \bar{g}_j)^2}$$

Figure of merit

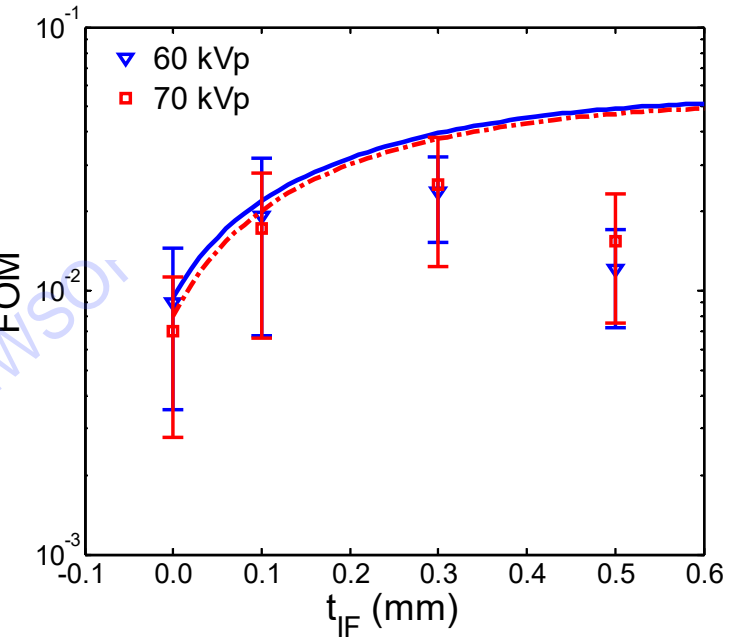
$$\text{FOM}_k = \frac{\text{CNR}_k^2}{X} = \frac{1}{X} \frac{C_k^2}{\sigma_k^2}$$

$$C_k = |w_{\hat{k}} \Delta \mu_{kM}^F - \Delta \mu_{kM}^R| t_k$$

$$w_{\hat{k}} = \frac{\Delta \mu_{\hat{k}M}^R}{\Delta \mu_{\hat{k}M}^F}$$

$$\sigma_k^2 = w_{\hat{k}}^2 \frac{\sigma_F^2}{d_F^2} + \frac{\sigma_R^2}{d_R^2} = \frac{w_{\hat{k}}^2}{\text{SNR}_F^2} + \frac{1}{\text{SNR}_R^2} \approx \frac{w_{\hat{k}}^2}{\bar{q}_0 X \textcolor{magenta}{A}_{eff,F} \text{DQE}_F(0)} + \frac{1}{\bar{q}_0 X \textcolor{magenta}{A}_{eff,R} \text{DQE}_R(0)}$$

$$\text{FOM}_k \approx (w_{\hat{k}} \Delta \mu_{kM}^F - \Delta \mu_{kM}^R)^2 t_k^2 \bar{q}_0 \left[\frac{w_{\hat{k}}^2}{A_{eff,F} \text{DQE}_F(0)} + \frac{1}{A_{eff,R} \text{DQE}_R(0)} \right]^{-1}$$



Scatter

$$C_k = |w_{\hat{k}} \Delta \mu_{kM}^F - \Delta \mu_{kM}^R| t_k$$

$$I(1 + \text{SPR}) = I_0 e^{-\sum_k \mu_k t_k}$$

$$C'_k = |C_k + \delta| t_k$$

$$\delta = \ln \left(\frac{1 + \text{SPR}_2^H}{1 + \text{SPR}_1^H} \right) - w_{\hat{k}} \ln \left(\frac{1 + \text{SPR}_2^L}{1 + \text{SPR}_1^L} \right)$$

Wrap-up

- We see a potential of microtomography with a sandwich detector for high-resolution bone-selective imaging without post-segmentation procedures
- Challenging issues are still remained for further quantitative imaging applications:
 - Halo effects
 - Preprocessing including the gain-offset correction
 - Trade-off between the contrast and noise
 - Trade-off between the energy separation and direct interaction-induced noise